Journal of Power Sources 250 (2014) 90–97

Contents lists available at ScienceDirect

Journal of Power Sources

journal homepage: www.elsevier.com/locate/jpowsour

Imidazolium-functionalized poly(ether ether ketone) as membrane and electrode ionomer for low-temperature alkaline membrane direct methanol fuel cell

Xiaoming Yan [a,b,c], Shuang Gu [d], Gaohong He [a,b,*], Xuemei Wu [a], Jay Benziger [c,**]

[a] State Key Laboratory of Fine Chemicals, Research and Development Center of Membrane Science and Technology, School of Chemical Engineering, Dalian University of Technology, Dalian, LN 116024, China
[b] School of Petroleum and Chemical Engineering, Dalian University of Technology, Panjin, LN 124221, China
[c] Department of Chemical and Biological Engineering, Princeton University, Princeton, NJ 08540, USA
[d] Department of Chemical and Biomolecular Engineering, University of Delaware, Newark, DE 19716, USA

HIGHLIGHTS

- Imidazolium-functionalized poly(ether ether ketone) was successfully synthesized.
- PEEK-ImOH HEMs exhibit improved dimensional stability.
- PEEK-ImOH HEMs exhibit high hydroxide conductivity (e.g., 52 mS cm^{-1} at 20 °C).
- PEEK-ImOH HEMs exhibit good mechanical property (e.g., 78 MPa of tensile strength).
- The methanol/O_2 fuel cell employing PEEK-ImOH shows high performance.

ARTICLE INFO

Article history:
Received 8 July 2013
Received in revised form
28 October 2013
Accepted 31 October 2013
Available online 8 November 2013

Keywords:
Imidazolium
Poly(ether ether ketone)
Ionomer
Alkaline anion exchange membrane
Alkaline membrane direct methanol fuel cell

ABSTRACT

A series of imidazolium-functionalized poly(ether ether ketone)s (PEEK-ImOHs) were successfully synthesized by a two-step chloromethylation–Menshutkin reaction followed by hydroxide exchange. PEEK-ImOH membranes with ion exchange capacity (IEC) ranging from 1.56 to 2.24 mmol g^{-1} were prepared by solution casting. PEEK-ImOHs show selective solubility in aqueous solutions of acetone and tetrahydrofuran, but are insoluble in lower alcohols. PEEK-ImOH membranes with IEC of 2.03 mmol g^{-1} have high hydroxide conductivity (52 mS cm^{-1} at 20 °C), acceptable water swelling ratio (51% at 60 °C), and great tensile strength (78 MPa), and surprising flexibility (elongation-to-break of 168%), and high thermal stability (Decomposition temperature: 193 °C). In addition, PEEK-ImOH membranes show low methanol permeability (1.3–6.9 × 10^{-7} cm^2 s^{-1}). PEEK-ImOH membrane was tested in methanol/O_2 fuel cell as both the HEM and the ionomer impregnated into the catalyst layer; the open circuit voltage is 0.84 V and the peak power density is 31 mW cm^{-2}.

1. Introduction

Low-temperature direct methanol fuel cells (DMFCs) are proposed as alternative power sources for portable applications [1]. Methanol is easily handled, has high energy density, and is widely availability. Most DMFCs have been based on proton exchange membranes (PEMs) [2–4]. However, PEM based DMFCs show sluggish electrode kinetics, substantial alcohol crossover and require high weight loading of precious metal catalysts which have hampered commercialization [5–7]. By switching the electrolyte from the acid to base, the electrode kinetics of low-temperature DMFC can be significantly enhanced [8–10]. Further, low-cost non-precious metals can be used as active catalysts (e.g. silver, nickel, and tin) [11–14]; these catalysts are also more durable [15–17]. The methanol crossover can be substantially reduced because hydroxide (OH^-) conduction opposes the methanol diffusion [8].

Hydroxide exchange membranes (HEMs) are the key components of low-temperature alkaline membrane DMFC (AMDMFC). HEMs

* Corresponding author. State Key Laboratory of Fine Chemicals, Research and Development Center of Membrane Science and Technology, School of Chemical Engineering, Dalian University of Technology, Dalian, LN 116024, China. Tel./fax: +86 411 84986291.
** Corresponding author. Tel.: +1 609 258 5416; fax: +1 609 258 0211.
E-mail addresses: hgaohong@dlut.edu.cn (G. He), benziger@princeton.edu (J. Benziger).

0378-7753/$ – see front matter © 2013 Elsevier B.V. All rights reserved.
http://dx.doi.org/10.1016/j.jpowsour.2013.10.140

serve as fuel/oxidant separators and hydroxide conductors [18,19]. High hydroxide conductivity, alcohol tolerance, and dimensional stability are critically required for high-performance HEMs in low-temperature AMDAMCs. Selective solubility is also required for HEM materials; they should be insoluble in alcohols but they should be soluble in low-boiling-point solvents that allow them to be cast as membranes and incorporated into catalyst layers, building efficient triple-phase-boundary necessary for high electrode performance.

Hydroxide conducting functional groups are responsible for the fundamental properties of HEMs, including solubility, conductivity, and stability [15,20]. Novel functional groups, e.g., quaternary phosphonium [15,21–23], guanidinium [24–27], and imidazolium [28–43], have been introduced to HEM materials to improve the solubility, conductivity, and/or stability. All three novel functional groups form polymer that are soluble in low-boiling-point solvents, facilitating processing to make membranes or incorporation into the catalyst layer. The imidazolium based HEM materials are unique in that they are insoluble in alcohols and their aqueous solutions. This desirable selective solubility makes the imidazolium functional group a great choice of developing high-performance HEMs for low-temperature AMDMFC.

The polymer matrix provide many other important HEM properties, including but not limited to dimensional stability, thermal stability, and mechanical property. Initially, aliphatic main-chain polymers (e.g., polyvinyl alcohol [29], poly(styrene–acrylonitrile–ethylene) [30], poly(ethylene methyl methacrylate) [31,34], and polystyrene [32,37]) were used to prepare imidazolium-functionalized HEMs. Subsequently aromatic main-chain polymers (e.g., polysulfone [28,33], bromomethylated poly(2,6-dimethyl-1,4-phenyleneoxide) [35], polyfluorene [39], and fluorinated poly(aryl ether oxadiazole)s [36]) were used. Among all the imidazolium-functionalized HEMs, imidazolium-functionalized polysulfone membranes show the highest hydroxide conductivity (53 mS cm^{-1} at 20 °C) [28], arising from its high ion exchange capacity (2.19 mmol g^{-1}). However, its dimensional stability and mechanical strength need improvement especially at elevated temperatures.

Enhancing the van der Waals interactions among polymer chains could improve dimensional stability [23]. Poly(ether ether ketone) (PEEK) has higher van der Waals interactions among polymer chains than PSf does. PEEK should be a good matrix to prepare an imidazolium-functionalized membrane with high conductivity, excellent alcohol tolerance, and good swelling resistance simultaneously. In this work, a series of imidazolium-functionalized PEEKs (PEEK-ImOHs) were synthesized through the simple and efficient Menshutkin reaction. Their properties of water uptake, dimensional stability, hydroxide conductivity, thermal stability, mechanical property, and methanol permeability were comprehensively investigated. Methanol/O_2 fuel cells employing imidazolium-functionalized polymer as both the HEM and the electrode ionomer were tested.

2. Experimental

2.1. Materials

Poly(ether ether ketone) (VESTAKEEP® 4000G) powder was provided by Evonik Degussa (China) Co. Ltd. Chloromethyl octylether (CMOE) was synthesized according to the method published in the Ref. [44]. Potassium hydroxide, H_2SO_4 (92.8%), methanol, ethanol, acetone, tetrahydrofuran (THF), and 1-methylimidazole (1-MIM) were obtained commercially and used as received without further purification. All the chemicals used were analytical purity grade. In order to reduce the effect of CO_2 on the membrane characterization, the deionized water was boiled to completely remove CO_2 prior to use.

2.2. Preparation of imidazolium hydroxide functionalized-PEEK (PEEK-ImOH) membranes

Imidazolium chloride-functionalized PEEK (PEEK-ImCl) was synthesized by the Menshutkin reaction between chloromethylated PEEK (CMPEEK) and 1-methylimidazole. CMPEEK was synthesized by the chloromethylation of PEEK using CMOE as chloromethylating agent and concentrated sulfuric acid as solvent, as described in our previous work [45]. Then 0.25 g CMPEEK was completely dissolved in 3 ml 1-methylimidazole at room temperature, followed by casting the solution onto a glass plate. During curing and drying of the cast film at 80 °C for 48 h, the CMPEEK reacted with 1-methylimidazole to form the imidazolium chloride-functionalized PEEK (PEEK-ImCl). The membrane was peeled off the glass plate when all the unreacted 1-methylimidazole solvent was evaporated. The PEEK-ImCl membrane was ion exchanged with 1 M KOH solution at room temperature for 48 h producing an imidazolium hydroxide-functionalized PEEK (PEEK-ImOH) membrane. The hydroxide exchanged membrane was immersed in deionized water in a sealed container for additional 48 h to completely remove the residual KOH. The synthetic and ion-exchanging processes are summarized in Fig. 1.

2.3. ^1H NMR

^1H NMR spectroscopy confirmed the synthesis of both CMPEEK and PEEK-ImCl; it was also used to determine the degree of chloromethylation (DC) of CMPEEK precursor. ^1H NMR spectra of 1-MIM, CMPEEK, and PEEK-ImCl were recorded on a Varian Unity Inova 400 spectrometer at a resonance frequency of 399.73 MHz. Circa 1 wt. % solutions of 1-MIM, CMPEEK, or PEEK-ImCl were prepared by dissolving them into DMSO-d_6. Tetramethylsilane (TMS) was used as an internal standard in all cases. The degree of chloromethylation (DC) of CMPEEKs was calculated from the NMR peak areas: DC = $2A(H_d)/A(H_c)$, where $A(H_d)$ and $A(H_c)$ are the integral area of the H_d peak and H_c peak in Fig. 2, respectively, as defined in our previous work [45].

2.4. Ion exchange capacity (IEC)

The IEC of the PEEK-ImOH membrane was measured by back titration. 0.2 g PEEK-ImOH membrane sample was equilibrated with 50 ml 0.01 M HCl standard solution for 24 h, followed by back titration of 0.01 M NaOH standard solution with phenolphthalein as the indicator. The measured IEC (IEC_m) of the PEEK-ImOH membrane was calculated by the following equation:

$$IEC_m = \frac{(V_b - V_s)\cdot C_{HCl}}{W_{dry}} \times 1000$$

where V_b and V_s are the consumed volumes (L) of the NaOH solution for the blank sample and the PEEK-ImOH membrane sample, respectively, C_{HCl} is the concentration (M) of HCl solution, and W_{dry} is the mass (g) of dry membrane sample.

2.5. Water uptake and swelling ratio

After ion exchange the PEEK-ImOH membrane was immersed into deionized water for more than 10 h. The weight and dimension (length and width) of the wet membrane were measured. Then the membrane was vacuum-dried at 50 °C for 12 h, and the weight and dimension of dry membrane were measured. The water uptake and swelling ratio were calculated by the two following equations, respectively:

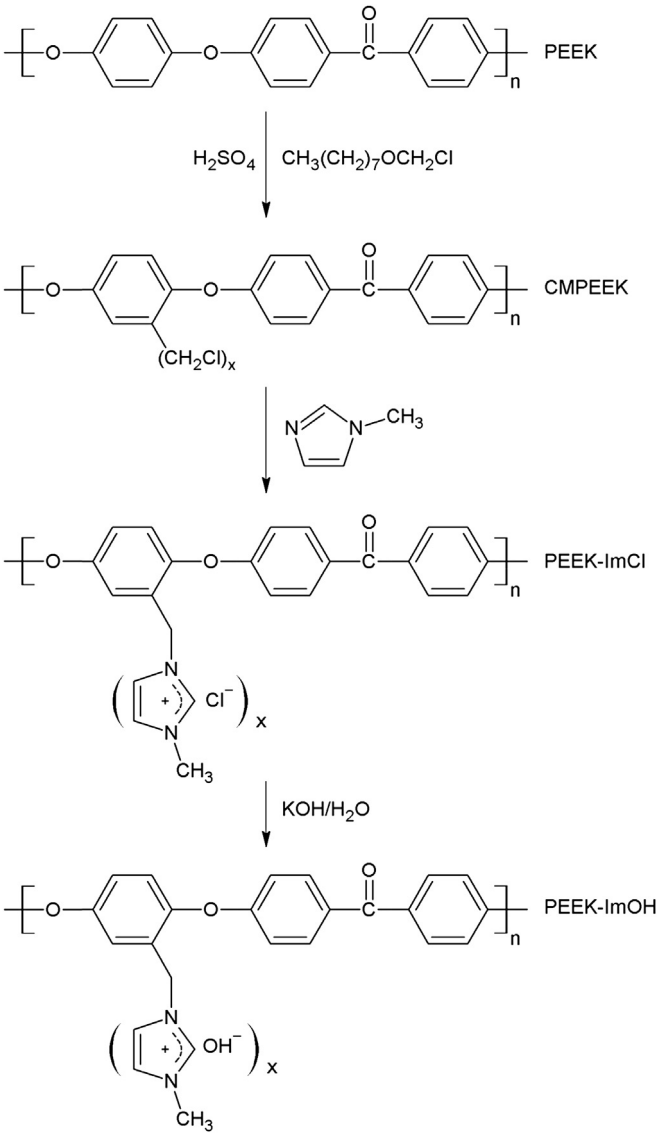

Fig. 1. Synthesis of the PEEK-ImOH.

$$\text{Water uptake}(\%) = \frac{W_{\text{wet}} - W_{\text{dry}}}{W_{\text{dry}}} \times 100$$

$$\text{Swelling ratio}(\%) = \frac{l_{\text{wet}} - l_{\text{dry}}}{l_{\text{dry}}} \times 100$$

where W_{wet} and W_{dry} are the mass of wet and dry membrane samples, respectively, l_{wet} and l_{dry} are the average length [$l_{\text{wet}} = (l_{\text{wet1}} \cdot l_{\text{wet2}})^{1/2}$, $l_{\text{dry}} = (l_{\text{dry1}} \cdot l_{\text{dry2}})^{1/2}$] of wet and dry membrane samples, respectively, in which, l_{wet1}, l_{wet2} and l_{dry1}, l_{dry2} are the lengths and widths of wet and dry membrane samples, respectively.

2.6. Small-angle X-ray scattering (SAXS)

SAXS analysis of the membrane samples was carried out by using PANalytical X'Pert Powder X-ray diffraction system. The intensity of the X-ray scattering was plotted versus the scattering vector, q, defined as $4\pi\sin\theta/\lambda$, where λ is the X-ray wavelength of 0.154 nm.

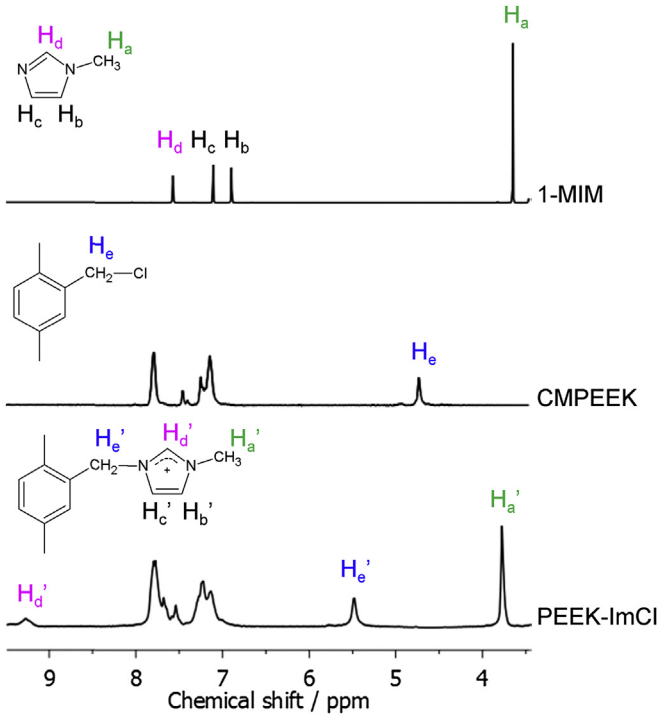

Fig. 2. ^{1}H NMR spectra of 1-MIM, CMPEEK (80%), and PEEK-ImCl (80%) (DMSO-d_6 as solvent).

2.7. Hydroxide conductivity

In-plane conductivity of the PEEK-ImOH membranes was measured by a typical four-electrode AC impedance method with membranes completely immersed in deionized water. The measurement apparatus consists of two platinum foils as the current carriers and two platinum wires as the potential sensors. Through plane conductivity was measured for membranes in saturated water vapor (100% RH in nitrogen gas). An Ivium Technologies Impedance Analyzer was used to measure AC impedance from 1 to 10^6 Hz. Prior to the gas phase measurements, all the membranes were fully hydrated in deionized water for 24 h. The hydroxide conductivity, σ, of the membrane was calculated through the following equation:

$$\sigma = \frac{L}{WdR}$$

where L is the distance between the two potential electrodes (1 cm here), d and W are the thickness and width of the membrane sample, respectively, and R is the high frequency resistance.

2.8. Mechanical property

The tensile modulus and strain at break of the dry and hydrated membranes were obtained with a SANS mechanical analyzer in an air atmosphere at room temperature with the cross-head speed of 5 mm min^{-1}. Dumbbell-shaped membrane samples were tailored following the international standard ISO 527.

2.9. Thermogravimetric analysis (TGA)

A TGA analyzer (Mettler Toledo TGA/SDTA851^e) was used to test the thermal stability of the PEEK-ImOH. About 10 mg sample was heated from 100 to 700 °C at a heating rate of 10 °C min^{-1} under an air atmosphere (air flow rate: 80 mL min^{-1}). The samples were

dried for 24 h at 50 °C in vacuum to remove moisture prior to the test. Derivative thermogravimetry (DTG) curve is the first order differential of the TGA curve on temperature.

2.10. Methanol permeability

Membrane methanol permeability was determined from transient transport. A membrane, effective area 2.27 cm^2, was clamped between two stirred cells (A, B). Cell A ($V_A = 20$ ml) was filled with a solution of methanol (1 M) and 1-butanol (0.02 M) in deionized water. Cell B ($V_B = 20$ ml) was filled with a 1-butanol (0.02 M) solution in deionized water. The butanol served as an internal standard for gas chromatographic analysis. The concentration of methanol in cell B was measured as a function of time by withdrawing 3 μl samples for analysis by a Shimadzu GC-14B gas chromatograph. Methanol permeability P was determined from taking the slope of the line of C_B vs. time, t.

$$C_B(t) = \frac{A}{V_B}\frac{P}{L}C_A(t - t_0)$$

V_B is the volume of cell B (L), A and L are the area (cm^2) and thickness (cm) of the membrane sample, respectively, P ($cm^2\ s^{-1}$) is the methanol permeability, $C_B(t)$ is the concentration in compartment B at time t, C_A is the concentration in compartment A and t_0 is the relaxation time for methanol to absorb into the membrane.

2.11. Fuel cell test

Catalyst coated membranes were prepared with catalyst ink consisting of 40 mg platinum black (E-TEK), 8 mg PEEK-ImOH 80% (0.5 g 5 wt.% PEEK-ImOH solution in 50 vol./50 vol. acetone–water), 1 g DI water, and 1 g acetone. Catalyst ink for Nafion 212 MEAs was prepared by mixing the 40 mg platinum black (E-TEK), 8 mg Nafion (0.5 g 5 wt.% Nafion solution in 50 vol./50 vol. *n*-propanol–water), 1 g DI water, and 1 g *n*-propanol. The catalyst inks were sonicated at room temperature for 10 min before use. The electrodes (both anode and cathode) were prepared by spraying the catalyst ink onto the membranes to the desired Pt loading of 0.5 mg Pt cm^{-2}. Carbon cloth gas diffusion layers (E-TEK) were used at both the anode and cathode sides. The membranes electrode assembly (MEA) has 1 cm^2 active area. The MEA was assembled in a single cell fixture for the fuel cell tests. *I–V* polarization curves were obtained at room temperature with anode feed of 10 mL min^{-1} 2 M methanol solution and cathode feed of 20 mL min^{-1} pure O_2.

3. Result and discussion

3.1. ^1H NMR confirmation

^1H NMR spectra of 1-methylimidazole, CMPEEK, and PEEK-ImCl are shown in Fig. 2. 1-methylimidazole spectrum shows four proton signals: 3.63 ppm (methyl, H_a), 6.88 and 7.09 ppm (ethylene in imidazole ring, H_b and H_c), and 7.56 ppm (methylene in imidazole ring, H_d). The CMPEEK spectrum has a single-peak at 4.72 ppm (methylene in chloromethyl group, H_e) and one group of peaks at 7.15–7.81 ppm from the aromatic rings. Detailed attributions were reported in our previous work [45]. After the Menshutkin reaction between CMPEEK and 1-methylimidazole, the proton signal of methylene in imidazole ring shifted from 7.56 ppm (H_d) to 9.28 ppm (H_d'). Formation of imidazolium considerably increases the acidity of its methylene protons, downshifting their signal significantly. The formation of imidazolium also shifted the proton signal of the methyl substituent slightly change from 3.63 ppm in 1-methylimidazole (H_a) to 3.78 ppm in imidazolium group (H_a'). At the same time, the proton signal of methylene shifted from 4.72 ppm (H_e) in CMPEEK to 5.48 ppm (H_e') in PEEK-ImCl. The NMR signature confirmed that PEEK-ImCl had been successfully synthesized, and that all of the chloromethyl groups in CMPEEKs had been converted to the imidazolium groups. These results are consistent with high reactivity for the Menshutkin reaction between 1-methylimidazole molecule and chloromethyl previously reported by our group [28].

3.2. Ion exchange capacity and solubility

Ion exchange capacity (IEC) is strongly correlated with HEM properties, such as water uptake, swelling ratio, hydroxide conductivity, and methanol permeability. The theoretical maximum IEC (IEC_t) and measured IEC (IEC_m) of PEEK-ImOH membranes with different degrees of chloromethylation (DCs) are listed in Table 1. IEC_t was calculated, based on the assumption of the complete conversion of the chloromethyl group in CMPEEK to imidazolium hydroxide groups: $IEC_t = 1000DC/(M_{PEEK} + 112.1DC)$, where DC is the degree of chloromethylation of CMPEEK and M_{PEEK} is the molecular weight of PEEK repeating unit (288.3 g mol^{-1}). For convenience, the PEEK-ImOH membrane is denoted as PEEK-ImOH xx%, where xx% is the DC of CMPEEK precursor. As expected, the IEC_m of PEEK-ImOH increases remarkably from 1.56 to 2.24 mmol g^{-1} with DC from 60% to 90%. All of IEC_ms are slightly lower than, but over-all very close to, the theoretical ones (IEC_t: from 1.69 to 2.31 mmol g^{-1}).

The solubility of PEEK-ImOHs in four typical low-boiling-point water-soluble solvents and their aqueous solutions were tested and the results are shown in Table 2. As expected, similar to the PSf-ImOHs described in our previous work [28], all the PEEK-ImOHs are insoluble in methanol, ethanol, and their aqueous solutions. PEEK-ImOHs are insoluble in neat acetone and THF, but they are soluble in aqueous solutions of acetone and THF (e.g., 50 vol.%).

3.3. Thermal stability

TGA and DTG curves of PEEK-ImOH are shown in Fig. 3. PEEK-ImOH has two weight loss steps: The first step at $T_{max\ rate} = 261$ °C has a 20 wt.% weight loss. That mass loss is approximately the mass fraction of 1-methylimidazole in PEEK-ImOH (17.4 wt.%), suggested that the observed weight loss is most likely ascribed to the removal of 1-methylimidazole. Imidazole removal by an S_N2 nucleophilic substitution by OH^- at the methylene–carbon links between imidazolium ring and polymer benzene ring have been reported by Awad et al. [46] The second step at $T_{max\ rate} = 604$ °C has a 24 wt.% of weight loss is suggested to be associated with removal of the residual side chain (hydroxymethylene group formed after imidazole removal) and the decomposition of main-chain. The high thermal stability of PEEK-ImOH, onset of decomposition, T_{OD}: 193 °C, is sufficient for HEM applications (typically, 60 °C of working temperature [47]).

Table 1
IEC of PEEK-ImOH membranes.

Membrane	DC/%	Thickness/μm	IEC_t/mmol g^{-1}	IEC_m/mmol g^{-1}
PEEK-ImOH 60%	60	95	1.69	1.56
PEEK-ImOH 68%	68	98	1.87	1.73
PEEK-ImOH 74%	74	92	1.99	1.91
PEEK-ImOH 80%	80	95	2.12	2.03
PEEK-ImOH 90%	90	101	2.31	2.24

Table 2
Solubility of PEEK-ImOHs in low-boiling-point solvents.

PEEK-ImOH membrane	Acetone	50 vol.% acetone in water	THF	50 vol.% THF in water	Methanol	50 vol.% methanol in water	Ethanol	50 vol.% ethanol in water	Water
PEEK-ImOH 60%	−	+	−	+	−	−	−	−	−
PEEK-ImOH 68%	−	+	−	+	−	−	−	−	−
PEEK-ImOH 74%	−	+	−	+	−	−	−	−	−
PEEK-ImOH 80%	−	+	−	+	−	−	−	−	−
PEEK-ImOH 90%	−	+	−	+	−	−	−	−	−

+: Soluble; −: Insoluble.

3.4. Water uptake and swelling ratio

Water uptake is essential for hydroxide conductivity, methanol permeability, and it also affects the mechanical property of HEMs [48]. Water uptakes of PEEK-ImOH membranes at different temperatures are shown in Fig. 4. Water uptake increases with IEC; water uptake increases more than linearly with IEC. Increasing hydroxide substitution from 74% to 80% increased water uptake from 61% to 159%. The high water uptake at 80% substitution is suggested to result from reduced mechanical strength of the polymer matrix.

SAXS spectra of PEEK-ImOH membranes are shown in Fig. 5. The intensity of the ionomer peak is much greater for PEEK-ImOH 80% membrane than for PEEK-ImOH 74% membrane (IEC: 2.03 vs. 1.91 mmol g^{-1}), which indicates that PEEK-ImOH 80% membrane has more ordering of the hydrophilic domains at the higher IEC.

The swelling ratios of the PEEK-ImOH membranes in water at different temperatures are shown in Fig. 6. Similar to the water uptake, the swelling ratio also increases with increasing both IEC and temperature. All the PEEK-ImOH membranes are flexible and robust, and most of their swelling ratios are below 50%. Swelling is limited by the balance of the energy of solvation of the ionic groups and the energy to expand the polymer matrix. Higher IEC will reduce inter-chain interactions of PEEK-ImOH membrane reducing the energy penalty for membrane swelling.

For all PEEK-ImOH membranes, the water uptake is almost constant from 20 to 50 °C and then increases abruptly between 50 and 60 °C. This behavior has been previously observed with proton exchange membranes [49]. The SAXS spectra of PEEK-ImOH 80% membrane also showed the intensity of ionomer peak increases significantly after swelling at 60 °C.

The swelling ratios of PEEK-ImOH and PSf-ImOH membranes [28] at 60 °C are compared in Fig. 7. At the same IEC PEEK-ImOH shows lower swelling ratio than PSf-ImOH. The difference in swelling behavior may arise from the inter-chain interactions in PEEK and PSf. Enhanced van der Waals interaction among polymer chains decreases swelling [23].

3.5. Mechanical property

Mechanical properties of fuel cell membranes are important, especially for the fuel cell durability, since variations in temperature and humidity can cause cyclic stresses and strains (mechanical loading) in the membrane during the fuel cell operation. The tensile strength and elongation-to-break of PEEK-ImOH, PSf-ImOH, and Cr-PVStAN-ImOH membranes with the similar swelling ratio are listed in Table 3. The PEEK-ImOH membrane exhibits better mechanical property than PSf-ImOH. In the wet state, PEEK-ImOH and PSf-ImOH membranes have tensile strengths 18 vs. 4 MPa and elongation-to-break 167% vs. 32% respectively. In the dry membrane state, the tensile strengths are 78 vs. 18 MPa and elongation-to-break 168% vs. 167% of elongation-to-break. The mechanical properties of PEEK-ImOH membrane are also better than that of Cr-PVStAN-ImOH crosslinked membrane (11 MPa of tensile strength

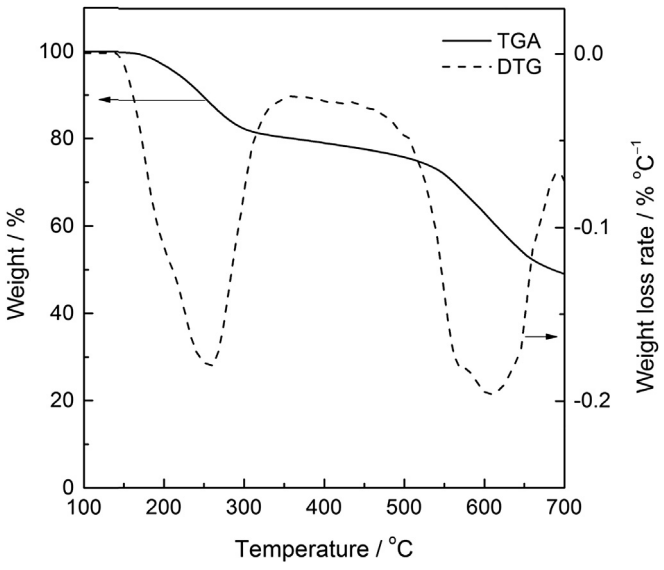

Fig. 3. TGA and DTG curves of PEEK-ImOH 80%.

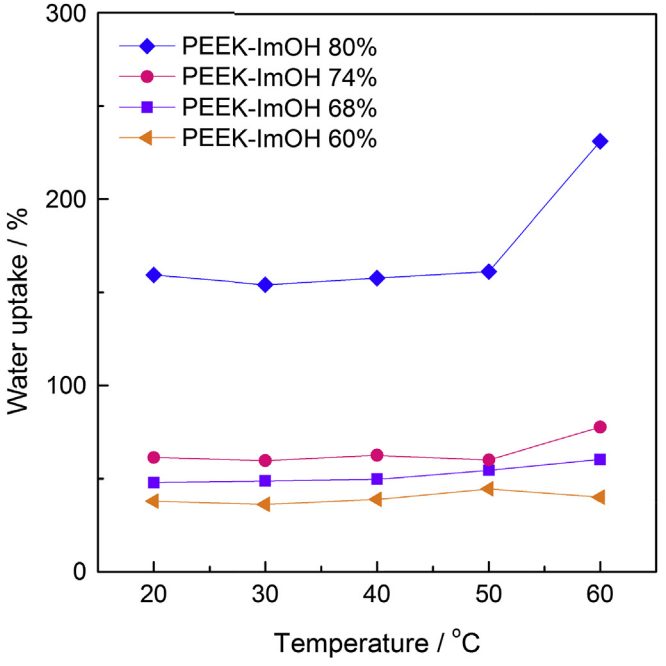

Fig. 4. Water uptake of PEEK-ImOH membranes at different temperatures.

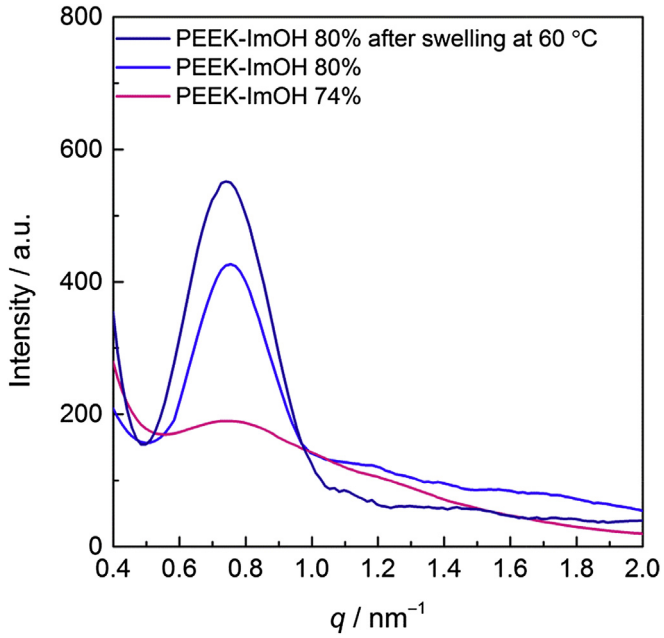

Fig. 5. SAXS spectra of PEEK-ImOH membranes.

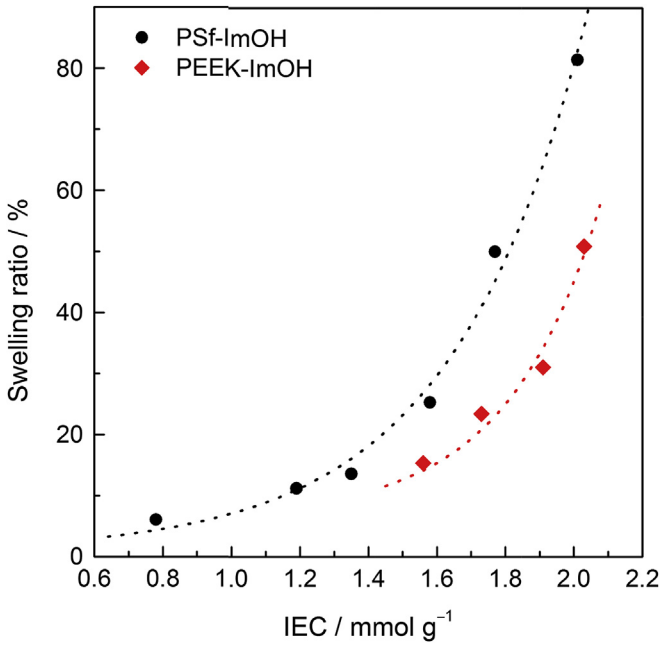

Fig. 7. Swelling ratio (60 °C) of PEEK-ImOH and PSf-ImOH membranes.

and 136% of elongation-to-break), in spite of the crosslinking techniques used.

3.6. Hydroxide conductivity

Hydroxide conductivities of PEEK-ImOH membranes as functions of IEC are shown in Fig. 8. The in-plane and through-plane hydroxide conductivities both increase remarkably with increasing IEC. The in-plane conductivity is higher than the through-plane conductivity. The possible reason is that the water uptake of the membrane is higher in water than in nitrogen gas with RH of 100% (e.g. 159% vs. 65% for PEEK-80% membrane). The hydroxide conductivity is significantly higher for PEEK-ImOH 80% membrane (52 mS cm^{-1}) than for quaternary ammonium functionalized one (17 mS cm^{-1} for PEEK-QAOH 76% that was the most conductive PEEK-QAOH membrane) [45]. The imidazolium cation appears to be superior to the traditional quaternary ammonium cation. The conductivity of PEEK-ImOH (52 mS cm^{-1}) is also higher than those of all the other imidazolium-functionalized membranes (10–42 mS cm^{-1} [28–41]). The excellent properties of PEEK-ImOH membranes suggest that PEEK is a good choice for HEM polymer matrices.

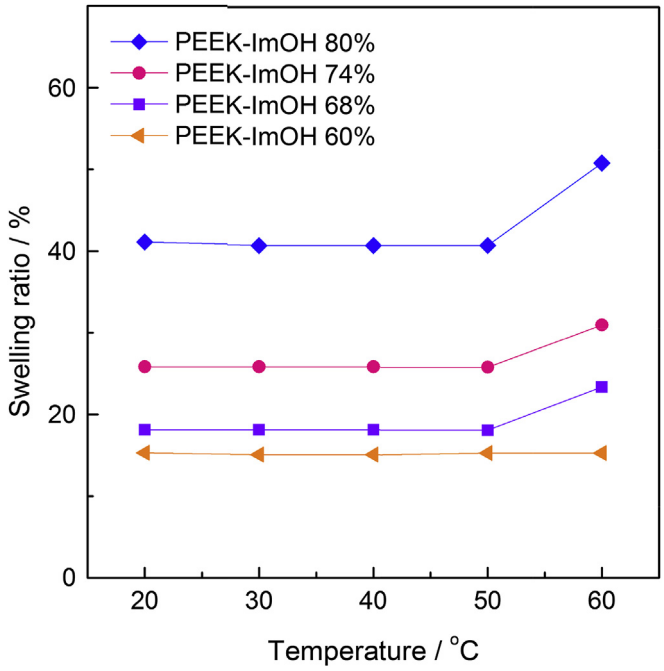

Fig. 6. Swelling ratio of PEEK-ImOH membranes at different temperatures.

Hydroxide conductivity of the PEEK-ImOH membrane dramatically increases with temperature, as seen in Fig. 9. At 60 °C, the PEEK-ImOH 80% membrane exhibits a conductivity of 77 mS cm^{-1}. Based on the Arrhenius relationship between ionic conductivity and temperature, the apparent activation energies (ΔE_as) of hydroxide conductivity were calculated to be 11.1, 10.2 and 8.8 kJ mol^{-1} for PEEK-ImOH 60%, PEEK-ImOH 74% and PEEK-ImOH 80% membranes, respectively. ΔE_a decreases with increasing IEC. There appears to be an inverse correlation between water uptake and the activation energy for hydroxide conductivity.

3.7. Methanol permeability and methanol/O_2 fuel cell performance

Low methanol permeability is essential for alcohol fuel cell membranes. Methanol permeabilities of PEEK-ImOH membranes are shown in Fig. 10. Methanol permeability (at 20 °C) of PEEK-ImOH membrane increases from 1.3×10^{-7} to 6.9×10^{-7} cm^2 s^{-1} with increasing IEC from 1.56 to 2.03 mmol g^{-1}. Even at the highest IEC the methanol permeabilities of PEEK-ImOH membranes are 1/10 to 1/50 that of Nafion 212 membrane (6.5×10^{-6} cm^2 s^{-1}) under the same test conditions. Furthermore, owing to the opposing fluxes of hydroxide and methanol, the methanol crossover in practical fuel cells is expected to be further lowered.

Polarization curves of a methanol/O_2 fuel cell with PEEK-ImOH 80% are presented in Fig. 11. PEEK-ImOH was used as both the membrane and the ionomer in the catalyst layers. The open circuit voltage of methanol/O_2 fuel cell with PEEK-ImOH is 0.84 V, which is

Table 3
Mechanical property of ImOH-functionalized HEMs with the similar swelling ratio.

Membrane	IEC/mmol g^{-1}	Swelling ratio/%	Tensile strength and (elongation-to-break)/MPa and (%)		Ref.
			Wet state	Dry state	
PEEK-ImOH 80%	2.03	41	18 (167)	78 (168)	This work
PSf-ImOH 132%	2.19	41	4 (32)	N/A	This work
Cr-PVStAN-ImOH (crosslinked)	N/A	47	11 (136)	N/A	[30]

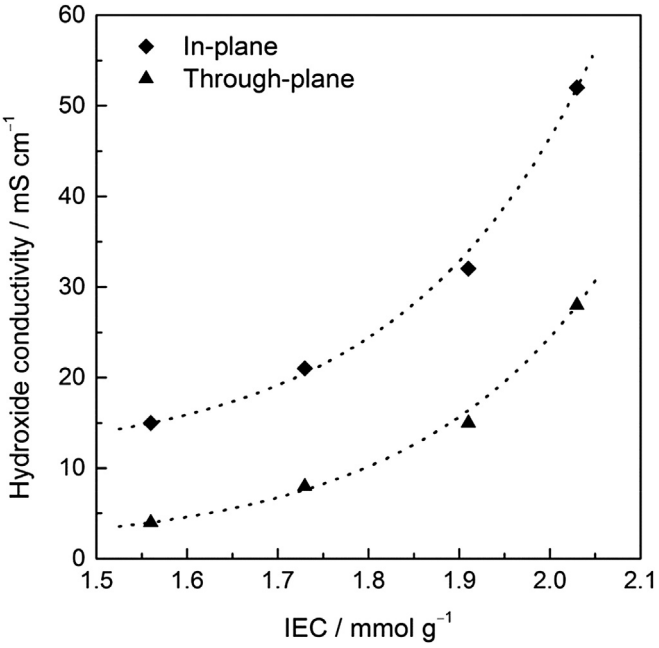

Fig. 8. Hydroxide conductivity of PEEK-ImOH membranes depending on IEC.

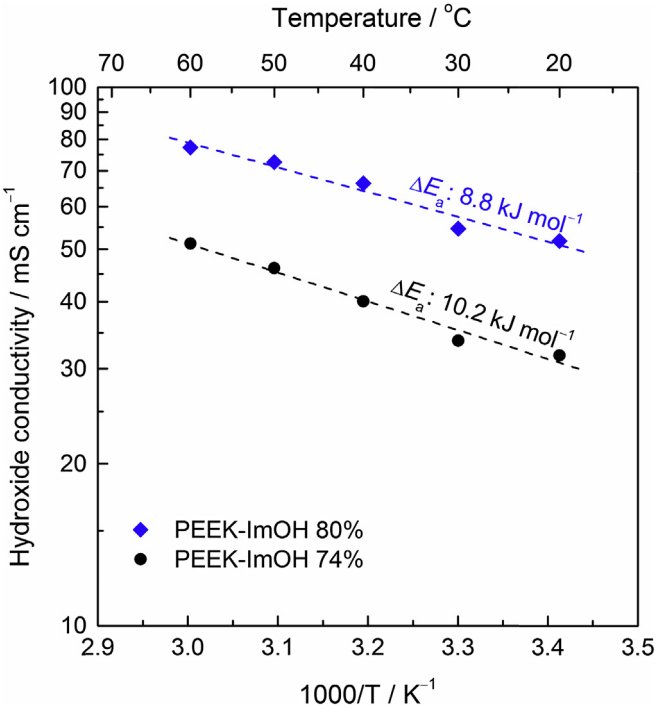

Fig. 9. Hydroxide conductivity of PEEK-ImOH membranes at different temperatures.

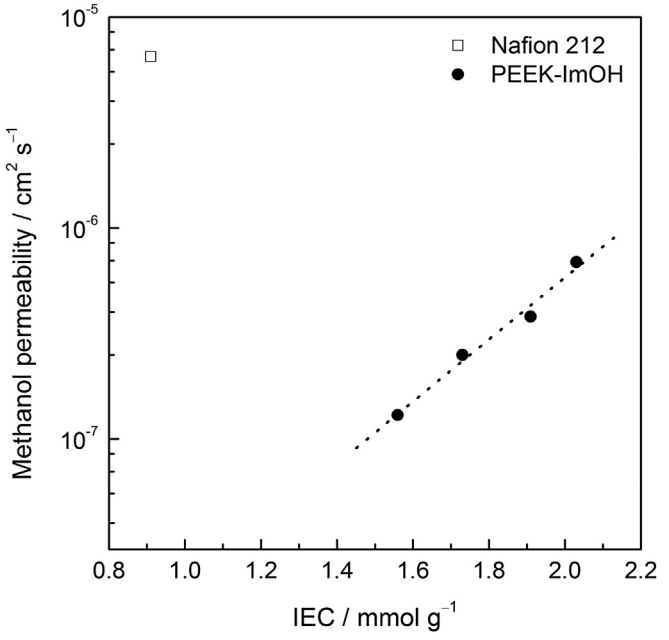

Fig. 10. Methanol permeability (20 °C) of PEEK-ImOH membranes against the IEC.

higher than that with Nafion 212 membrane as well as other HEMs (0.35–0.63 V [50–54]). Reduced methanol crossover of PEEK-ImOH reduces the voltage drop. The methanol/O_2 fuel cell with PEEK-ImOH exhibits a peak power density of 31 mW cm^{-2}. Although it is lower than that with Nafion 212 membrane (42 mW cm^{-2}), it is

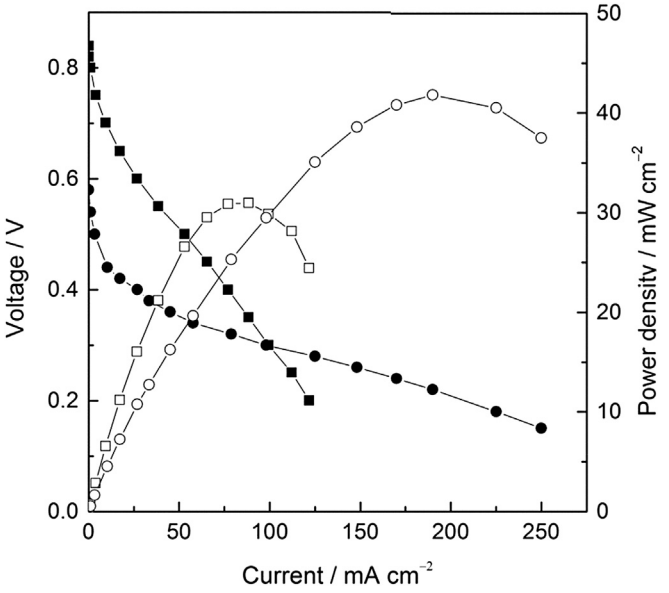

Fig. 11. Polarization curve (filled symbols) and power density curve (empty symbols) of a methanol/O_2 fuel cell with PEEK-ImOH at room temperature.

higher than those with other HEMs reported (0.0076–7 mW cm^{-2} [50–54]). The improved performance of fuel cells with PEEK-ImOH are attributed to the high conductivity of PEEK-ImOH, and more efficient three-phase-boundary in the catalyst layer resulting from incorporating PEEK-ImOH as the ionomer in the catalyst layers.

4. Conclusions

A series of soluble imidazolium-functionalized poly(ether ether ketone)s (PEEK-ImOHs) were synthesized by the chloromethylation–Menshutkin reaction two-step method. PEEK-ImOHs show desirable selective solubility; they are soluble in aqueous solutions of acetone or tetrahydrofuran, and insoluble in aqueous alcohols (e.g., methanol and ethanol). Ion exchange capacity (IEC) of PEEK-ImOH membranes ranges from 1.56 to 2.24 mmol g^{-1} with degree of chloromethylation from 60% to 90%. PEEK-ImOH membranes exhibit high hydroxide conductivity, e.g., PEEK-ImOH 80% membrane with IEC of 2.03 mmol g^{-1} has hydroxide conductivity of 52 mS cm^{-1} at 20 °C. This value is higher those of all the imidazolium-functionalized HEMs previously reported (10–42 mS cm^{-1}). PEEK-ImOH membranes exhibit good swelling resistance (swelling ratio of $\leq$51% even at 60 °C). With the same swelling ratio, PEEK-ImOH 80% membranes show better mechanical property than PSf-ImOH 132% membranes and Cr-PVStAN-ImOH membranes (tensile strength of 18 vs. 4 and 11 MPa, and elongation-to-break of 167% vs. 32% and 136%) in the wet state. PEEK-ImOH 80% membranes exhibit enhanced tensile strength (78 MPa) and good flexibility (elongation-to-break of 168%) in the dry state. PEEK-ImOH membrane possesses sufficient thermal stability for use in fuel cells (T_{OD}: 193 °C). In addition, PEEK-ImOH membranes have low methanol permeabilities (1.3–6.9 $\times$ 10^{-7} cm^2 s^{-1}), which are 1/10–1/50 that of Nafion 212 membrane. The methanol/O_2 fuel cell employing the PEEK-ImOH as both the HEM and the electrode ionomer displays a high open circuit voltage of 0.84 V and a high peak power density of 31 mW cm^{-2} at room temperature.

Acknowledgments

The authors thank the support of National Science Fund for Distinguished Young Scholars of China (Grant No. 21125628) and National Natural Science Foundation of China (Grant No. 21176044).

References

[1] Y. Wang, K.S. Chen, J. Mishler, S.C. Cho, X.C. Adroher, Appl. Energy 88 (2011) 981–1007.
[2] S. Bose, T. Kuila, X.L.N. Thi, N.H. Kim, K.T. Lau, J.H. Lee, Prog. Polym. Sci. 36 (2011) 813–843.
[3] A. Chandan, M. Hattenberger, A. El-Kharouf, S.F. Du, A. Dhir, V. Self, B.G. Pollet, A. Ingram, W. Bujalski, J. Power Sources 231 (2013) 264–278.
[4] X.L. Li, A. Faghri, J. Power Sources 226 (2013) 223–240.
[5] R. Borup, J. Meyers, B. Pivovar, Y.S. Kim, R. Mukundan, N. Garland, D. Myers, M. Wilson, F. Garzon, D. Wood, P. Zelenay, K. More, K. Stroh, T. Zawodzinski, J. Boncella, J.E. McGrath, M. Inaba, K. Miyatake, M. Hori, K. Ota, Z. Ogumi, S. Miyata, A. Nishikata, Z. Siroma, Y. Uchimoto, K. Yasuda, K.I. Kimijima, N. Iwashita, Chem. Rev. 107 (2007) 3904–3951.
[6] S. Basri, S.K. Kamarudin, W.R.W. Daud, Z. Yaakub, Int. J. Hydrogen Energy 35 (2010) 7957–7970.
[7] X.W. Zhou, Y.L. Gan, J.J. Du, D.N. Tian, R.H. Zhang, C.Y. Yang, Z.X. Dai, J. Power Sources 232 (2013) 310–322.
[8] E. Antolini, E.R. Gonzalez, J. Power Sources 195 (2010) 3431–3450.
[9] V. Bambagioni, C. Bianchini, A. Marchionni, J. Filippi, F. Vizza, J. Teddy, P. Serp, M. Zhiani, J. Power Sources 190 (2009) 241–251.
[10] Y.-S. Ye, M.-Y. Cheng, X.-L. Xie, J. Rick, Y.-J. Huang, F.-C. Chang, B.-J. Hwang, J. Power Sources 239 (2013) 424–432.
[11] H. Bunazawa, Y. Yamazaki, J. Power Sources 190 (2009) 210–215.
[12] F. Bidault, A. Kucernak, J. Power Sources 196 (2011) 4950–4956.
[13] J. Kim, T. Momma, T. Osaka, J. Power Sources 189 (2009) 999–1002.
[14] J. Kim, T. Momma, T. Osaka, J. Power Sources 189 (2009) 909–915.
[15] S. Gu, R. Cai, T. Luo, Z.W. Chen, M.W. Sun, Y. Liu, G.H. He, Y.S. Yan, Angew. Chem. Int. Ed. 48 (2009) 6499–6502.
[16] K. Matsumoto, T. Fujigaya, H. Yanagi, N. Nakashima, Adv. Funct. Mater. 21 (2011) 1089–1094.
[17] J. Pan, S.F. Lu, Y. Li, A.B. Huang, L. Zhuang, J.T. Lu, Adv. Funct. Mater. 20 (2010) 312–319.
[18] G. Merle, M. Wessling, K. Nijmeijer, J. Membr. Sci. 377 (2011) 1–35.
[19] C.G. Arges, V. Ramani, Proc. Natl. Acad. Sci. U. S. A. 110 (2013) 2490–2495.
[20] C. Arges, V. Ramani, J. Electrochem. Soc. 160 (2013) F1006–F1021.
[21] S. Gu, R. Cai, T. Luo, K. Jensen, C. Contreras, Y.S. Yan, ChemSusChem 3 (2010) 555–558.
[22] S. Gu, R. Cai, Y.S. Yan, Chem. Commun. 47 (2011) 2856–2858.
[23] S. Gu, J. Skovgard, Y.S. Yan, ChemSusChem 5 (2012) 843–848.
[24] Q.A. Zhang, S.H. Li, S.B. Zhang, Chem. Commun. 46 (2010) 7495–7497.
[25] J.H. Wang, S.H. Li, S.B. Zhang, Macromolecules 43 (2010) 3890–3896.
[26] D.S. Kim, A. Labouriau, M.D. Guiver, Y.S. Kim, Chem. Mater. 23 (2011) 3795–3797.
[27] L. Xiaocheng, W. Liang, L. Yanbo, O. Ai Lien, S.D. Poynton, J.R. Varcoe, X. Tongwen, J. Power Sources 217 (2012) 373–380.
[28] X.M. Yan, G.H. He, S. Gu, X.M. Wu, L.G. Du, Y.D. Wang, Int. J. Hydrogen Energy 37 (2012) 5216–5224.
[29] X.L. Zhu, B.A. Wang, H.P. Wang, Polym. Bull. (Berlin) 65 (2010) 719–730.
[30] B.C. Lin, L.H. Qiu, J.M. Lu, F. Yan, Chem. Mater. 22 (2010) 6718–6725.
[31] M.L. Guo, J. Fang, H.K. Xu, W. Li, X.H. Lu, C.H. Lan, K.Y. Li, J. Membr. Sci. 362 (2010) 97–104.
[32] W. Li, J. Fang, M. Lv, C.X. Chen, X.J. Chi, Y.X. Yang, Y.M. Zhang, J. Mater. Chem. 21 (2011) 11340–11346.
[33] F.X. Zhang, H.M. Zhang, C. Qu, J. Mater. Chem. 21 (2011) 12744–12752.
[34] Y.S. Ye, Y.A. Elabd, Macromolecules 44 (2011) 8494–8503.
[35] J. Ran, L. Wu, J.R. Varcoe, A.L. Ong, S.D. Poynton, T.W. Xu, J. Membr. Sci. 415 (2012) 242–249.
[36] Q.H. Hu, Y.M. Shang, Y.W. Wang, M. Xu, S.B. Wang, X.F. Xie, Y.G. Liu, H.L. Zhang, J.H. Wang, Z.Q. Mao, Int. J. Hydrogen Energy 37 (2012) 12659–12665.
[37] B. Qiu, B.C. Lin, L.H. Qiu, F. Yan, J. Mater. Chem. 22 (2012) 1040–1045.
[38] B. Qiu, B.C. Lin, Z.H. Si, L.H. Qiu, F.Q. Chu, J. Zhao, F. Yan, J. Power Sources 217 (2012) 329–335.
[39] B.C. Lin, L.H. Qiu, B. Qiu, Y. Peng, F. Yan, Macromolecules 44 (2011) 9642–9649.
[40] A.H.N. Rao, R.L. Thankamony, H.-J. Kim, S. Nam, T.-H. Kim, Polymer 54 (2013) 111–119.
[41] B. Lin, H. Dong, Y. Li, Z. Si, F. Gu, F. Yan, Chem. Mater. 25 (2013) 1858–1867.
[42] O.I. Deavin, S. Murphy, A.L. Ong, S.D. Poynton, R. Zeng, H. Herman, J.R. Varcoe, Energy Environ. Sci. 5 (2012) 8584–8597.
[43] D.Y. Chen, M.A. Hickner, ACS Appl. Mater. Interfaces 4 (2012) 5775–5781.
[44] A. Warshawsky, A. Deshe, J. Polym. Sci. Part A Polym. Chem. 23 (1985) 1839–1841.
[45] X.M. Yan, G.H. He, S. Gu, X.M. Wu, L.G. Du, H.Y. Zhang, J. Membr. Sci. 375 (2011) 204–211.
[46] W.H. Awad, J.W. Gilman, M. Nyden, R.H. Harris, T.E. Sutto, J. Callahan, P.C. Trulove, H.C. DeLong, D.M. Fox, Thermochim. Acta 409 (2004) 3–11.
[47] J.R. Varcoe, R.C.T. Slade, Fuel Cells 5 (2005) 187–200.
[48] X.M. Wu, G.H. He, S. Gu, Z.W. Hu, X.M. Yan, Chem. Eng. J. (Lausanne) 156 (2010) 578–581.
[49] S. Gu, G.H. He, X.M. Wu, C.N. Li, H.J. Liu, C. Lin, X.C. Li, J. Membr. Sci. 281 (2006) 121–129.
[50] A.B. Huang, C.Y. Xia, C.B. Xiao, L. Zhuang, J. Appl. Polym. Sci. 100 (2006) 2248–2251.
[51] H.W. Zhang, Z.T. Zhou, J. Appl. Polym. Sci. 110 (2008) 1756–1762.
[52] K. Scott, E. Yu, G. Vlachogiannopoulos, M. Shivare, N. Duteanu, J. Power Sources 175 (2008) 452–457.
[53] A. Santasalo-Aarnio, S. Hietala, T. Rauhala, T. Kallio, J. Power Sources 196 (2011) 6153–6159.
[54] C.C. Yang, S.S. Chiu, S.C. Kuo, T.H. Liou, J. Power Sources 199 (2012) 37–45.